

# Equivalence between top-down and bottom-up holographic approaches

Miguel Angel Martin Contreras\* and Mitsutoshi Fujita†

*School of Nuclear Science and Technology  
University of South China  
Hengyang, China  
No 28, West Changsheng Road,  
Hengyang City, Hunan Province, China.*

Alfredo Vega‡

*Instituto de Física y Astronomía,  
Universidad de Valparaíso,  
A. Gran Bretaña 1111, Valparaíso, Chile*

This work raises the question of whether finding an equivalent bottom-up description to a given top-down one is possible. We consider the vector meson spectrum derived in the D3/D7 system to answer this question. Using WKB analysis, we reconstruct a bottom-up confining potential that resembles the geometric structure of the so-called hardwall model. We compute some properties for this bottom-up model, including the thermal deconfinement phase transition, the  $\rho$  radial Regge trajectory, and the configurational entropy.

## I. INTRODUCTION

AdS/CFT correspondence [1] since its original formulation has become an excellent tool to address non-perturbative phenomena beyond gravitational physics. After almost twenty-five years of effective models, all of them can be classified into two main groups, regarding how they are *defined*: top-down and bottom-up.

Top-down models, roughly speaking, are constructed *systematically* from a well-defined string theory, leading to a holographically consistent gauge theory. In other words, we are dealing with an entire gauge/gravity duality framework, assuming we have complete knowledge of both sides, allowing exact predictions based on known theories. Therefore, the top-down approach is mainly used to test and refine the AdS/CFT correspondence.

Conversely, the bottom-up approach studies and understands AdS/CFT by starting with specific, well-defined components and building a more comprehensive understanding. This customization allows for more flexibility than the bottom-up case. However, the payback of such an approach is that bottom-up models are effective models, restricted by their phenomenological framework. A good example is the plethora of research works about AdS/QCD.

In the particular case of holographic QCD, both perspectives have been used to address hadronic spectroscopy. However, the mechanism to induce confinement, *ergo* the emergence of bounded states, varies in each paradigm. In the top-down case, deforming the geometry induces naturally an energy scale setting hadron masses [2]. For the bottom-up case, confinement is induced by breaking the bulk conformal symmetry but

keeping the AdS conformally flat limit exhibited by the bulk modes dual to hadrons at the boundary. However, this procedure can be done by deforming the AdS space [3–6] or inducing a dilaton field [7]. Both scenarios allow the emergence of bulk-bound states dual to hadrons.

This fact allows us to ask if it is possible to find a bottom-up model that captures some of the properties of a top-down one. And the preliminary answer is yes. The key point is the hadronic spectrum: *given a hadronic spectrum, we can always use WKB to find the associated confining potential and, therefore, an associated dilaton.* This technique comes from molecular physics, the Rydberg [8, 9] – Klein [10] – Rees [11] (RKR) method, a well-known semi-classical procedure used to derive a potential for the Schrödinger equation based on the energy spectrum. In this manuscript, we will exploit this idea.

This work is organized as follows: Section II briefly introduces the bottom-up description of hadrons. Section III introduces the concepts behind the WKB method for reconstructing potentials from boundary Regge trajectories. As an illustrative example, we reconstruct the static quadratic dilaton, i.e., the Softwall model [7]. In Section IV, we argue that the D3/D7 top-down model can be approached as a bottom-up Hardwall model. We substantiate this claim by performing a WKB reconstruction starting from the D3/D7 mass spectrum. Section V discusses the confinement/deconfinement phase transition, following the well-known analysis by Herzog [12]. Section VI addresses the configurational entropy for vector mesons computed within the WKB reconstructed framework. Finally, we present our conclusions in Section VII.

## II. MESONS IN BOTTOM-UP MODELS

In the bottom-up approach, mesons are defined using the normalizable bulk modes that emerge when we use a confinement scale that breaks conformal invariance in

\* miguelangel.martin@usc.edu.cn

† fujitamitsutoshi@usc.edu.cn

‡ alfredo.vega@uv.cl

the bulk. We use a dilaton field  $\Phi(z)$  that can be static or dynamically generated. Along with the dilaton, we have to set a geometric frame. It is customary to work on the *Poincare Patch* defined as

$$dS^2 = \frac{R^2}{z^2} (dz^2 + \eta_{\mu\nu} dx^\mu dx^\nu), \quad (1)$$

where  $R$  is the AdS radius,  $z$  is the so-called *holographic coordinate* and  $\eta_{\mu\nu}$  is the Minkowski metric that describes the conformal boundary at  $z \rightarrow 0$ .

The bulk action in this kind of model is given as usual as

$$I_{\text{Mesons}} = \frac{1}{g_5^2} \int d^5x \sqrt{-g} e^{-\Phi(z)} \mathcal{L}_{\text{Mesons}}, \quad (2)$$

with  $g_5$  a scale that fixes units in the action and also helps to define the decay constants [5]. The Lagrangian density for the 1-form bulk fields (dual to mesons) can be summarized as

$$\mathcal{L}_{\text{Hadrons}} = -\frac{1}{2} \nabla_m \phi^n \nabla^m \phi_n + \frac{1}{2} M_5^2 \phi^n \phi_n. \quad (3)$$

The bulk mass  $M_5$  plays an important role in the bottom-up approach. This quantity defines the *hadronic identity* associated with the bulk modes. From the field/operator duality, the dimension  $\Delta$  of operators creating mesons at the boundary is dual to the scaling of the bulk fields in the limit  $z \rightarrow 0$ . For mesons, we can write this dimension as  $\Delta = 3+l$ , since operators defining mesons have structures  $\mathcal{O} = f(\bar{q}, q, D_\mu)$ . The derivatives introduce *angular momentum* for angular excitations. In this scenario, the bulk mass is defined as

$$M_5^2 R^2 = \frac{1}{4} (3 + 2l - \beta) (1 + 2l + \beta) \quad (4)$$

where  $\beta = -(3 - 2S)$  characterizes the meson spin. For scalar fields,  $\beta = -3$ , and for vector fields,  $\beta = -1$ .

In general, the bulk action defines a *Sturm-Liouville* equation obtained after Fourier transforming and redefining the bulk field as  $\phi_m(z, q) = \tilde{\phi}_m(q) \psi(z, q)$ , with  $\tilde{\phi}_m$  defined as a polarization vector. This equation for the bulk field  $\psi(z, q)$  has the structure

$$\partial_z \left[ e^{-B(z)} \partial_z \psi(z, q) \right] + (-q^2) e^{-B(z)} \psi(z, q) - \frac{M_5^2 R^2}{z^2} e^{-B(z)} \psi(z, q) = 0. \quad (5)$$

where we have defined  $B(z) = \Phi(z) + \beta \log\left(\frac{R}{z}\right)$  and  $-q^2 = M_n^2$  is the on-shell condition. The meson spectrum  $M_n^2$  emerges from the equation above. However, it is customary to transform the Sturm-Liouville equation into a Schrodinger-like equation that is characterized by

the emergence of a *holographic potential* whose eigenspectrum is the Regge trajectory for mesons characterized by the dilaton field  $\Phi(z)$ .

To do so, we define the *Bogoliubov transformation*  $\psi(z) = e^{\frac{1}{2}\Phi(z)} u(z)$  such that the Sturm-Liouville equation reduces to the expected Schrodinger-like equation:

$$-u''(z) + V(z) u(z) = M_n^2 u(z), \quad (6)$$

with the holographic potential defined in terms of the dilaton and the AdS warp factor as

$$V(z) = \frac{M_5^2 R^2}{z^2} - \frac{\beta(2-\beta)}{4z^2} - \frac{\beta}{2z} \Phi'(z) + \frac{1}{4} \Phi'(z)^2 - \frac{1}{2} \Phi''(z). \quad (7)$$

By solving this potential, we obtain the mass spectrum. This potential will be the starting point in the next section.

### III. WKB RECONSTRUCTION

A possible form to address the inverse Schrödinger problem is to use the WKB approach. Suppose we have a hadronic Regge trajectory from experimental fits or proposed from non-holographic models that can be written as a function of the excitation number, i.e.,  $M_n^2(n)$ .

The fundamental question underlying this inverse problem relies on what kind of phenomenology is described from the large  $z$  behavior of the potential. In other words, the large  $z$  behavior will determine the large  $z$  profile of the dilaton. In the case of the Regge trajectories, this is enough to describe them. The large  $z$  behavior in the holographic potential controls the Regge trajectory linearity and slope. The low  $z$  limit gives the intercept.

We learned from the original Softwall [7] that the holographic potential large  $z$  behavior controls confinement naturally. In the case of top-down approaches, the equivalent of large  $z$  behavior *conveniently* deforms the bulk space and bulk fields to induce a mass of excited states dual to mesons, as in the D3/D7 approach [13].

The main idea is to extract the static dilaton from the Regge trajectory. To do so, we will consider a general trajectory defined as

$$M_n^2(n) = f(a_i, n), \quad (8)$$

where  $a_i$  defines a set of parameters, i.e., energy scales, that fix the units in the trajectory. For example, for heavy mesons, it is expected that trajectories do not exhibit linearity [14]; or for large distances in Cornell-like potential, the emergence of a Coulomb-like spectrum is expected.

As explained in Appendices A and B, the large  $z$  behavior of the potential near the turning points can be inferred using the WKB approximation using one of the formulas of the RKR method. Since the conformal boundary is at  $z \rightarrow 0$ , for holographic potentials the turning points are  $z \rightarrow 0$  and  $z(V^*)$  with the property that  $z(V^*) \rightarrow \infty$ , thus we have

$$z(V^*) = 2 \int_0^{V^*} \frac{dM^2}{\frac{dM^2}{dn} (V^* - M^2)^{1/2}}. \quad (9)$$

Inverting this expression, we find the high- $z$  potential responsible for confinement in bottom-up models. The near-conformal boundary behavior of the potential and dilaton controls the behavior of decay constants, as was exposed in refs. [15, 16]. We use  $V^*$  to denote the potential calculated using WKB from the full bottom-up holographic potential  $V(z)$ , which can be written as

$$V(z) = \frac{\beta(\beta - 2) + 4M_5^2 R^2}{4z^2} + V^*(z), \quad (10)$$

where the hadronic identity is encoded in the bulk mass  $M_5$ . An important remark should be made at this point. Even though we use a given Regge trajectory or mass spectrum, the equivalent bottom-up potential does not fit the input spectrum. The ground states could be slightly deviated. High precision is expected in the excited states. However, this is solved by fine-tuning.

Once we have the equivalent bottom-up potential from the spectrum, we can calculate the associated dilaton field  $\Phi(z)$ . To do so, we use reverse engineering on the potential  $V^*(z)$  as follows:

$$V^*(z) = \frac{1}{4}\Phi'(z)^2 - \frac{1}{2}\Phi''(z) - \frac{\beta}{2z}\Phi'(z). \quad (11)$$

At low  $z$ , the holographic potential is not sensitive to the dilaton since, in this region,  $\Phi(z \rightarrow 0)$  is expected to converge softly to a constant value.

The strength of this prescription comes from the treatment of experimental Regge trajectories.

### A. Softwall model

The Softwall model is characterized by linear Regge trajectories, i.e.,  $M^2(n) = a(n + b)$ . In this case (9) produces:

$$z(V^*) = 2 \int_0^{V^*} \frac{dM^2}{a(V^* - M^2)^{1/2}} = \frac{4}{a}\sqrt{V^*}. \quad (12)$$

Therefore, the large  $z$  differential equation has the following structure:

$$\frac{1}{16}a^2 z^2 = \frac{1}{4}\Phi'(z)^2 - \frac{1}{2}\Phi''(z) + \frac{1}{2z}\Phi'(z), \quad (13)$$

where we have fix  $\beta = -1$  for vector mesons.

Solving the equation above, we obtain for the dilaton the following expression:

$$\Phi(z) = c_1 - 2 \log \left[ \cosh \left( \frac{a}{8}z^2 - 2c_2 \right) \right]. \quad (14)$$

For the argument inside the logarithm function, we can write:

$$\cosh \left( \frac{a}{8}z^2 - 2c_2 \right) = \cosh \frac{a}{8}z^2 \cosh 2c_2 - \sinh \frac{a}{8}z^2 \sinh 2c_2. \quad (15)$$

Fixing  $c_1 = 0$  and  $c_2 \rightarrow \infty$ , implying that  $\cosh 2ac_2 = \sinh 2ac_2 = 1$ . Therefore, we obtain an expression for the dilaton field coming from boundary information as follows

$$\Phi(z) = -2 \log \left( e^{-\frac{a}{8}z^2} \right) = \frac{a}{4}z^2 \quad (16)$$

If we compare with the standard Softwall model, where  $\Phi(z) = \kappa^2 z^2$ , we can infer the dilaton slope in terms of the Regge slope as  $\kappa^2 = a/4$ . This fact immediately implies that we recover the well-known result coming from linear confinement for the vector Regge trajectories at  $S$ -wave:

$$M_n^2 = 4\kappa^2(n + 1). \quad (17)$$

Thus, we have recovered the Softwall model. The results for scalar mesons can be obtained similarly by fixing  $\beta = -3$ .

## IV. BOTTOM-UP APPROACH TO D3/D7 MODEL

Let us apply these WKB ideas to the D3/D7 model in a top-down approach [17, 18]. Two types of D-branes in this model are considered non-perturbative solitonic objects, characterized by their tension and energy being inversely proportional to the string coupling constant, denoted as  $1/g_s$ , which is unlike fundamental strings. Specifically, D7-branes are separate from D3-branes along a perpendicular direction.  $L$  is the distance between the D3 and the D7 branes that sets the mass scale of fluctuations.

Flavor information is obtained by intersecting  $N_c$  D3 branes with  $N_f$  D7 branes in Minkowski space. In the appropriate decoupling limit and requiring  $g_s N_c \gg 1$ , the stack of D3-branes can be replaced with the  $\text{AdS}_5 \times \text{S}_5$  geometry with the AdS throat radius  $R^2 = \sqrt{4\pi g_s} N_c \alpha'$

. If, in addition, condition  $N_c \gg N_f$  is imposed, it is possible to neglect the backreaction of D7-branes, which implies that in the gravity description, they appear as  $N_f$  D7-brane probes. This process implies breaking the original  $\mathcal{N} = 4$  supersymmetry into a  $\mathcal{N} = 2$  one, allowing one to include dynamical quark fields analogous to QCD. Recall that quark fields transform in the fundamental representation of the gauge group, while  $\mathcal{N} = 4$  theory only contains fields in the adjoint representation. Thus, the  $\mathcal{N} = 2$  theory acquires a spectrum of mesons.

Geometrically speaking, the mesons in this model arise as fluctuations of the associated DBI action. These D7-brane plane wave fluctuations form a set of massive gauge supermultiplets of the  $\mathcal{N} = 2$  theory. We can identify with mesons the modes with conformal dimension  $\Delta = l + 3$ . For these modes, the mass spectrum has the structure:

$$M_{n,l}^2 = \frac{4L^2}{R^4} (n + l + 1)(n + l + 2) \quad (18)$$

The mass spectrum is entirely dominated by the large  $z$  terms in the potential. Thus, from WKB, we can infer the bottom-up counterpart of this D3/D7 spectrum. Applying the WKB integral, we have:

$$\begin{aligned} z(V^*) &= 2 \int_0^{V^*} \frac{dM_{n,l}^2}{\frac{\partial M_{n,l}^2}{\partial n} (V^* - M_{n,l}^2)^{1/2}} \\ &= 2 \int_0^{V^*} \frac{dM_{n,l}^2}{a \sqrt{1 + \frac{4M_{n,l}^2}{a}} \sqrt{V^* - M_{n,l}^2}} \\ &= \frac{2}{\sqrt{a}} \tan^{-1} \left( 2 \sqrt{\frac{V^*}{a}} \right), \end{aligned} \quad (19)$$

where we have defined the energy scale  $a = 4L^2/R^4$  that sets the meson masses.

Inverting the equation above, we obtain the large  $z$  part of the bottom-up potential as

$$V^*(z) = \frac{a}{2} \tan^2 \left( \frac{\sqrt{a}z}{2} \right). \quad (20)$$

Therefore, the bottom-up potential equivalent to the D3/D7 model for mesons acquires the following structure:

$$V_{\text{D3/D7}}(z) = \frac{(2l+3)(2l+1)}{4z^2} + \frac{a}{4} \tan^2 \left( \frac{\sqrt{a}z}{2} \right). \quad (21)$$

Let us dissect this potential. First, we focus our attention on functional behavior. The potential has a periodic structure controlled by the scale  $a = 4L^2/R^4$ . Thus, the potential will go to infinity when

$$z_{\text{cutoff}} = \frac{\pi}{\sqrt{a}} (2\gamma + 1) = \frac{\pi R^2}{2L} (2\gamma + 1), \quad \gamma \in \{0, \mathbb{N}\}. \quad (22)$$

Thus,  $z_{\text{cutoff}}$  defines a *wall* that prevents modes from going beyond these points. For simplicity, we will fix  $\gamma = 0$ . This observation leads us to the second point. *This confining potential has the same behavior as the one observed for the Hardwall model* [5, 19]. A phenomenological fact supports this claim. The Hardwall model spectrum is defined by the zeroes of Bessel functions of the first kind as

$$M_n^2 = \left( \frac{\alpha_{1,n}}{z_{\text{HW}}} \right)^2, \quad (23)$$

where the energy scale is fixed by the locus  $z_{\text{HW}}$  of the D-brane used to cut the AdS slice. Therefore, the geometrical effect of intersecting a stack of D3-branes with another one of D7-branes living in a 10-dimensional Minkowski separated by a distance  $L$  is *equivalent* to slice the AdS<sub>5</sub> space with a hard cutoff. In both scenarios, the meson mass depends entirely on distance: in the D3/D7 case,  $L$ , and the Hardwall model case,  $z_{\text{HW}}$ . And both scenarios have the same behavior of the spectrum:  $M_n^2 \propto n^2$ .

Thus, we can conclude that the bottom-up potential (21) *mimics* the spectroscopy of the D3/D7 system, which is a top-down scenario.

### 1. Fixing parameters

For simplicity, we can write the D3/D7 trajectory for S-wave mesons as

$$M_n^2 = a(n+1)(n+2), \quad \text{with: } a = \frac{4L^2}{R^4}. \quad (24)$$

We will focus our attention on the light-vector mesons. To do so, we identify the  $\rho(770)$  meson as the ground state with  $n = 0$ , and its mass to fix the energy scale  $a$  as

$$M_{\rho(770)}^2 = 2a, \quad \text{thus: } a = 0.3 \text{ GeV}^2 \quad (25)$$

This energy scale will allow us to compute the mass spectrum, thermal structure, and configurational entropy to characterize this *reconstructed* bottom-up model. A plot of the reconstructed potential  $V(z)$ , with the setup of the parameters, is given in Fig. 1.

### 2. Dilaton Reconstruction

To find the dilaton field associated with the bottom-up D3/D7 potential, we will require as boundary conditions that  $\Phi(z \rightarrow 0) = 0$  and

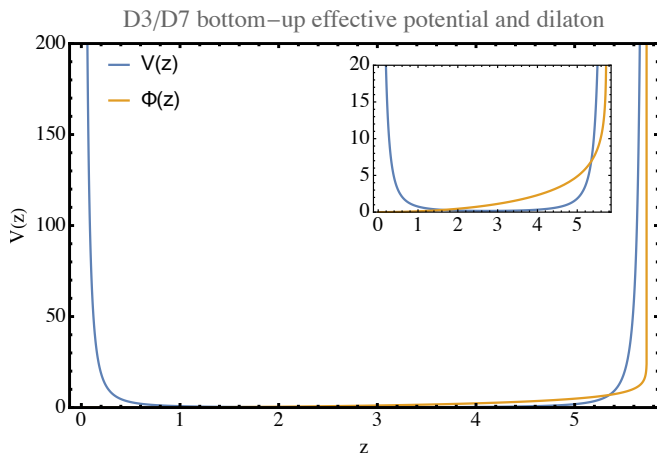


FIG. 1. Reconstructed bottom-up potential from the D3/D7 meson spectrum and the corresponding static dilaton. Notice that the dilaton diverges asymptotically at *wall* located at  $z = \pi/\sqrt{a}$ . We have used the  $\rho(770)$  meson mass to fix parameters according to eqn. (25). Experimental masses come from PDG [20].

$$\Phi(z^* \rightarrow \infty) = 2 \int^{z^*} dz \sqrt{V_{\text{WKB}}(z)}, \quad (26)$$

with  $z^*$  a turning point in infinity. This set of conditions will allow us to solve the differential equation for the dilaton given in (11). A plot of this dilaton field  $\Phi(z)$  is depicted in Fig. 1.

Let us comment on the functional behavior of the dilaton. The dilaton in the region  $z \rightarrow 0$  goes to 0. However, in the vicinity of  $z = \pi/\sqrt{a}$ , the dilaton diverges. Thus, the dilaton is effectively *confined spatially*. In the bulk action, this characteristic will cause the bulk dynamics to be restricted, i.e., the quantity  $\pi/\sqrt{a}$  behaves as a wall. Thus,  $a$  is a *confinement scale* in the same sense as  $\kappa$  in the Softwall model [7].

### A. Holographic spectrum of the Reconstructed Potential

Let us focus in this part on the holographic spectrum associated with the potential (21) when we consider vector mesons in  $s$ -wave.

As usual in the bottom-up approach, our starting point is to define the geometrical background. We will consider this system living in the Poincare patch given by the line element (1). Vector mesons are dual to vector massless bulk fields, obeying the following Lagrangian density:

$$\mathcal{L}_{\text{Meson}} = -\frac{1}{4g_5^2} F_{mn} F^{mn} \quad (27)$$

where  $F_{mn} = 2\partial_{(m} A_{n)}$ . Recall that for  $s$ -wave vector mesons, the bulk mass is fixed to the zero:  $M_5^2 R^2 = 0$ ,

Light Vector mesons $J^G(J^{PC}) = 1^+(1^{--})$				
Masses in MeV				
State	Exp.	HWM	D3/D7	Recons.
$\rho(770)$	$775.26 \pm 0.23$	775.23*	775.23*	796.02(2.7%)
$\rho(1450)$	$1465 \pm 25$	1779(21%)	1343(8%)	1368(7%)
$\rho(1700)$	$1720 \pm 20$	2790(62%)	1899(10%)	1926(11%)
$\rho(1900)$	$1880 \pm 10$	3801(102%)	2452(30%)	2480(32%)

TABLE I. Summary of vector meson masses for the  $\rho$  trajectory calculated using the Hardwall (HW), D3/D7 and reconstructed models. The asterisk (\*) indicates the experimental mass used to fix parameters in each model. For the reconstructed, we use the same value for the Regge slope  $a = 0.3 \text{ GeV}^2$  used in the D3/D7 case. Quantities inside parenthesis correspond to relative errors with experimental data [20].

since  $\Delta = 3$ , for vector mesons. Using this Lagrangian and the reconstructed dilaton plotted in Fig. 1, we can compute the Sturm-Liouville equation (6), given by

$$\partial_z \left[ e^{-B(z)} \psi(z, q) \right] + M_n^2 e^{-B(z)} A_\mu = 0, \quad (28)$$

and the corresponding Schrodinger-like equation given by

$$u''(z) + V_{\text{D3/D7}}(z) u(z) = M_n^2 u(z). \quad (29)$$

where we have performed the standard Bogoliubov transformation  $\psi(z) = e^{\frac{1}{2}B(z)} u(z)$ . The plot for the Schrodinger-like modes  $u_n(z)$ , and the Regge trajectories for the D3/D7 and the reconstructed WKB models are depicted in Fig. 2.

As we mentioned in the last section, for the D3/D7 system, we used the  $\rho$  meson mass to fix the slope  $a = 0.3 \text{ GeV}^2$ . This value was also used to fix the effective wall  $z_{\text{cutoff}}$ , according to the expression (22). The summary of the masses for the  $\rho$  radial trajectory is given in table I. We have compared the WKB reconstructed outcomes with the Hardwall and D3/D7. In the reconstructed case, the ground state  $\rho(770)$  emerges with a relative error smaller than 3%. The Hardwall model, which also obeys a quadratic in  $n$  behavior, increases faster than the D3/D7 and the reconstructed models since the behavior of the zeroes spectrum of the Bessel function of the first kind determines the masses. For higher excitations, the quadratic behavior deviates from the expected linear tendency observed for light-unflavored mesons.

## V. THERMAL HAWKING-PAGE TRANSITION

A useful test we can perform is analyzing the thermal phases associated with this D3-D7 inspired solution [12, 21]. In the AdS/CFT seminal works, Witten demonstrated that the thermodynamics of a gauge theory at the boundary is connected with the thermodynamics of AdS space. In particular, the Hawking-Page transition

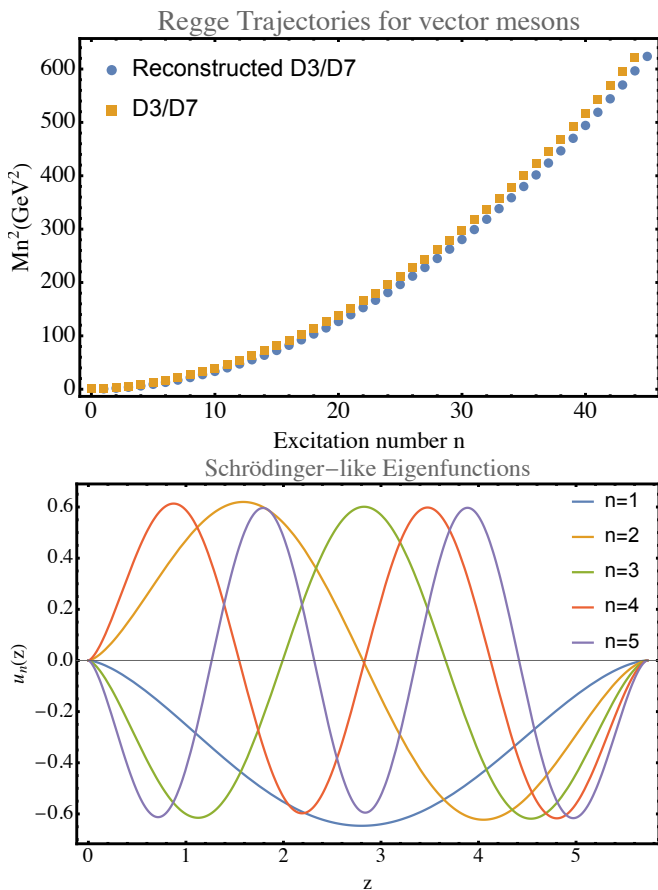


FIG. 2. The upper panel shows the radial Regge trajectories  $M_n^2$  for vector mesons in the D3/D7 system [2] and for the reconstructed one. The lower panel presents a plot of the ground state and the first four excited states for the reconstructed model.

in the bulk geometry carries information about the confinement/deconfinement process [12, 21]. The standard prescription is to compute the free energy in both solutions, the thermal AdS and the black hole one, AdSBH. These solutions are given by

$$dS_{\text{Th}}^2 = \frac{R^2}{z^2} [d\tau^2 + dz^2 + d\vec{x} \cdot d\vec{x}] \quad (30)$$

$$dS_{\text{BH}}^2 = \frac{R^2}{z^2} \left[ f(z) d\tau^2 + \frac{dz^2}{f(z)} + d\vec{x} \cdot d\vec{x} \right] \quad (31)$$

with  $f(z) = 1 - \frac{z^4}{z_h^4}$ , and  $z_h$  is the locus of the event horizon. The free energy is computed from the bulk action:

$$I = -\frac{1}{2\kappa^2} \int d^5x \sqrt{g} e^{-\Phi(z)} (\mathcal{R} - \Lambda) - \frac{1}{\kappa^2} \int_{\partial\mathcal{M}} d^4x \sqrt{h} e^{-\Phi(z)} \mathcal{K}, \quad (32)$$

evaluated on-shell using the thermal and AdS-BH solutions. We compute the free energy difference as  $\Delta F = F_{\text{Th}} - F_{\text{BH}}$  [22].

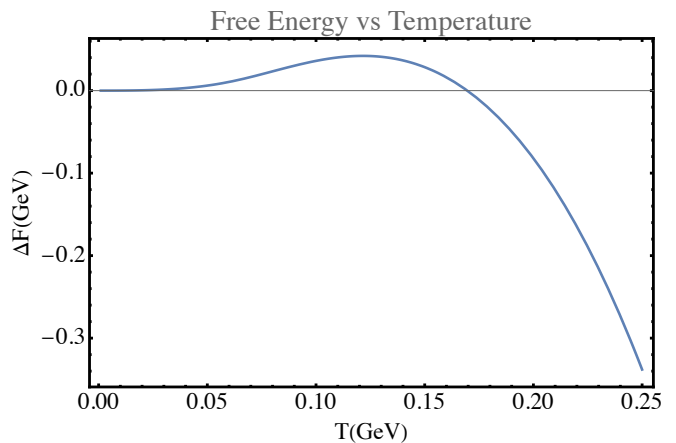


FIG. 3. Thermal Hawking-Page transition for the WKB reconstructed dilaton  $\Phi(z)$ , with  $a = 0.3$   $\text{GeV}^2$ . In this scenario, the confinement/deconfinement phase transition has a temperature of 169.6 MeV.

Notice that  $\kappa^2$  contains the information of the five-dimensional Newton constant,  $\mathcal{R}$  is the Ricci scalar,  $\Lambda$  is the cosmological constant,  $\mathcal{K}$  is the extrinsic curvature scalar, and  $h$  is the determinant of the boundary-induced metric. The last term in the action is necessary for regularization purposes [23]. Figure 3 depicts a plot of the bulk free energy difference for the WKB reconstructed dilaton.

From the Hawking-Page analysis, and keeping in mind the relation between the wall locus with the lightest vector meson in the Regge trajectory exposed by Herzog, for this WKB model, we found that for the critical temperature,

$$T_c = 0.169 \text{ GeV} = 0.218 m_\rho, \quad (33)$$

which is higher than the critical temperature of the Hard-wall model result,  $0.1574 m_\rho$ . However, this critical temperature is lower than the Softwall result  $0.2459 m_\rho$ . See [12].

## VI. CONFIGURATIONAL ENTROPY AND STABILITY

Configurational entropy (CE) is associated with the various arrangements (or microstates) that a specific macrostate can assume. Consequently, a higher CE signifies an increased number of potential microstate configurations. In thermodynamic terms, this entropy is connected with the work conducted by a system while remaining in a fixed spatial configuration, independent of any exchange of energy.

In information theory, configurational entropy (CE) is an important metric for assessing the relationship between the informational content of physical solutions and their corresponding equations of motion (e.o.m.). CE is

a logarithmic measure of the spatial complexity inherent in localized solutions given a specific energy content. Consequently, it quantifies the informational content embedded in the solutions to a particular set of equations of motion.

In more precise terms, CE can be viewed as an indicator of the degree of information required to describe how spatially localized the solutions to e.o.m. in the bulk are. Generally, dynamic solutions come from extremizing an action, and CE effectively measures the information available within these solutions.

In the framework of AdS/CFT, the holographic perspective on configurational entropy has been explored within both bottom-up and top-down AdS/QCD models [24]. The concept was initially introduced for the hadronic states in [25–30] and the associated references. Regarding the stability of heavy quarkonium, DCE was employed as a methodological tool to investigate thermal characteristics within a colored medium [31], considering the influence of magnetic fields [32] and finite density [33]. The study in [34] used CE to examine the holographic deconfinement phase transition within bottom-up AdS/QCD frameworks. Furthermore, recent research highlighted in [35] employs configurational entropy to analyze holographic stability in light nuclides. CE was also used to describe stable non- $q\bar{q}$  hadronic structures [36], isospectrality [37], and  $\Sigma$  baryons using bottom-up holography [38].

For systems exhibiting instability, we can posit that the configurational entropy contributes to a degree of stability. Generally, the hadronic mass can be expressed as a function that increases with configurational entropy. Furthermore, based on Heisenberg’s uncertainty principle, it is possible to define the decay width  $\Gamma$  concerning the hadron mass  $\Gamma \sim M_n \sim s_{\text{CE}}^\gamma$ , as referenced in [37]. Thus, for a holographic model that intends to describe hadrons, a *good phenomenological test* is the increase of the configurational entropy with the excitation number.

For vector hadrons, the recipe for configurational entropy  $s_{\text{CE}}$  can be summarized as follows:

1. Start from the bulk action (2) computing the equations of motion associated with the bulk fields dual to hadrons.
2. compute the on-shell energy-momentum tensor  $T_{mn}$ :

$$T_{mn} = \frac{2}{\sqrt{-g}} \frac{\partial [\sqrt{-g} \mathcal{L}_{\text{Hadron}}]}{\partial g^{mn}}. \quad (34)$$

3. Extract the  $T_{00}$  component, defined as the bulk energy density  $\rho(z)$ . For bulk vector fields,  $\rho(z)$  has the form:

$$\rho(z) = \frac{e^{-B(z)}}{2} \left( \frac{z}{R} \right)^3 \times \left\{ \left[ \frac{1}{\mathcal{K}^2} (M_n^2 \psi_n^2 + \psi_n'^2) - \frac{M_5^2 R^2}{z^2} \psi_n^2 \right] \right\} \Omega, \quad (35)$$

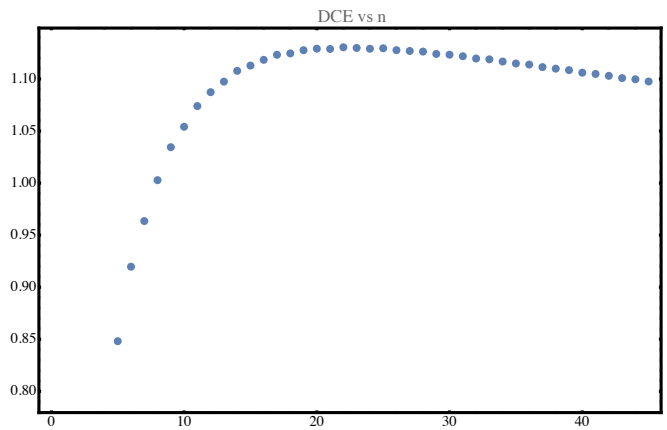


FIG. 4. Differential configurational entropy as a function of the excitation number  $n$  for vector mesons in the context of WKB reconstructed potential. For high enough  $n$ , DCE decreases.

where  $\Omega$  is a factor carrying plane wave and polarization contraction factors, which is irrelevant in the following calculation steps.

4. Fourier-transform the energy density  $\rho(z)$ :

$$\bar{\rho}(k) = \int_0^\infty dz e^{ikz} \rho(z) \quad (36)$$

and compute the *modal fraction* as

$$f(k) = \frac{|\bar{\rho}(k)|^2}{\int dk |\bar{\rho}(k)|^2}. \quad (37)$$

Recall that  $\rho(z) \in L^2(\mathbb{R})$ , and also has information on how energy is localized in the bulk. Thus, it indirectly measures how normalizable modes are well localized in the AdS space. Thus, the modal fraction measures the spread of the energy in the bulk.

5. Finally, compute the *differential configurational entropy* with the following prescription:

$$S_{\text{DCE}} = - \int dk \tilde{f}(k) \log \tilde{f}(k) \quad (38)$$

where  $\tilde{f}(k) = f(k) / f(k)_{\text{Max}}$ . Notice that we normalize the modal fraction with  $f(k)_{\text{Max}}$ .

We computed the differential configurational entropy (DCE) in natural units for the WKB reconstructed system for the first forty-five states. The calculation is depicted in Fig. 4. Notice that, as we expect from phenomenology, DCE increases for the first sixteen states. When we increase the excitation number, DCE decreases, as expected for the Hardwall model [37]. This suppression effect is associated with the presence of the wall, imposed by the  $\tan^2 az$  term that the holographic potential has, causes the *overlapping in the DCE* of the highest states with the lower ones. However, this behavior

is pathological in spaces with bounded geometries, as in the case of the Hardwall model.

## VII. CONCLUSIONS

This work is motivated by whether a top-down model has an equivalent bottom-up description. A simple form to address this query is to consider the mass spectrum obtained for hadrons in top-down models, since the mass spectrum is directly connected with the bottom-up holographic potential. Recall that, in bottom-up AdS/QCD, the mass spectrum is determined by the large- $z$  behavior of the holographic potential. Thus, by using WKB on the Regge trajectory, we can obtain the corresponding potential and dilaton field.

Applying this idea, we found that the D3/D7 model behaves as a hardwall-like model on the bottom-up side. This fact is unsurprising since meson masses in the D3-D7 case come from the consistent truncation of the geometry generated by the intersecting stacks of the D3 and D7 branes. Thus, the effective space where the solutions dual to mesons live is bounded. This picture is exactly the one expected in the Hardwall model. Therefore, roughly speaking, *a D3/D7 system can be seen as an effective Hardwall.*

We also tested the confinement/deconfinement phase transition for the reconstructed geometry. We found that the critical temperature is close to 169 MeV, higher than the usual Hardwall model.

Finally, we performed a configurational entropy analysis to test the feasibility of the reconstructed model to describe hadrons. We found that the configurational entropy is not an increasing function of  $n$  since it has a local maximum, as is expected for models like the Hardwall. However, for the lowest modes ( $n < 16$ ), CE increases with  $n$ , as we expected from phenomenological arguments. Thus, this reconstructed WKB model could describe light meson phenomena holographically.

## ACKNOWLEDGMENTS

M. A. Martin Contreras would like to acknowledge the financial support provided by the National Natural Science Foundation of China (NSFC) under grant No 12350410371.

### Appendix A: Summary of Rydberg-Klein-Rees procedure

The Rydberg [8, 9]-Klein [10]-Rees[11] method is a semiclassical inversion procedure for the Schrödinger equation that allows obtaining a bound state potential starting from an energy spectrum.

For the radial Schrödinger equation

$$-\frac{\hbar^2}{2m} \frac{d^2 u_E}{dr^2} + V(r)u_E = E u_E \quad (\text{A1})$$

According to the WKB approach, the quantization condition is

$$n + \frac{1}{2} = \frac{1}{\pi} \sqrt{\frac{2m}{\hbar^2}} \int_{r_1}^{r_2} \sqrt{E - V(r)} dr, \quad (\text{A2})$$

where  $n$  is the radial quantum number and  $r_{1,2}$  are the turning points.

The main result in the RKR method is two integrals which involve turning points (for details of the inversion procedure, see the appendix in [39]):

$$r_2 - r_1 = 2\sqrt{\frac{\hbar^2}{2m}} \int_{n_{min}}^n \frac{dn'}{\sqrt{E(n) - E(n')}} = 2f \quad (\text{A3})$$

$$\frac{1}{r_2} - \frac{1}{r_1} = 2\sqrt{\frac{\hbar^2}{2m}} \int_{n_{min}}^n \frac{B_{n'} dn'}{\sqrt{E(n) - E(n')}} = 2g, \quad (\text{A4})$$

the first equation, in the context of molecular physics, is called the vibrational RKR equation, and the second is rotational, with  $B_n$  is given by:

$$B_n = \left. \frac{\partial E(n, J)}{\partial [J(J+1)]} \right|_{J=0} \quad (\text{A5})$$

Then, from a well-known spectrum, RKR equations give us a collection of turning points, which can be interpolated to obtain a potential in this spectrum.

### Appendix B: Rydberg-Klein-Rees procedure for holography

In AdS/QCD models, we can always write the equation for AdS modes that describe hadrons as:

$$-u''(z) + V(z)u(z) = M_n^2 u(z), \quad (\text{B1})$$

with the holographic potential defined in terms of the dilaton and the AdS warp factor as:

$$V(z) = \frac{M_5^2 R^2}{z^2} - \frac{\beta(2-\beta)}{4z^2} - \frac{\beta}{2z} \Phi'(z) + \frac{1}{4} \Phi'(z)^2 - \frac{1}{2} \Phi''(z). \quad (\text{B2})$$

Here, the WKB quantization condition is:

$$n + \frac{1}{2} = \frac{1}{\pi} \int_{z_1}^{z_2} \sqrt{M^2 - V(z)} dz, \quad (\text{B3})$$



where  $n$  is the radial quantum number and  $z_{1,2}$  are the turning points.

We use  $V^*$  to denote the potential calculated using WKB from the full bottom-up holographic potential  $V(z)$ , which can be written as

$$V(z) = \frac{\beta(\beta - 2) + 4 M_5^2 R^2}{4 z^2} + V^*(z). \quad (\text{B4})$$

Comparing with B2,  $V^*(z)$  depends only on the dilaton field, and for large  $z$  gives the main contribution for higher states, so, in this case, we can approximate B2 by  $V^*(z)$  with turning points in zero and in  $z(V^*)$  to get mass spectra for radial excitations. This fact simplifies a lot our procedure because we can use the RKR method to obtain  $V^*(z)$  just considering A3, which in our case is:

$$z(V^*) = 2 \int_{n_{min}}^{n(M^2)} \frac{dn'}{\sqrt{M^2(n) - M^2(n')}} \quad (\text{B5})$$

As  $M^2 = M^2(n)$ , we can change the integration variable in the last integral by considering that in the turning points, we have  $M^2(n) = V^*$  and  $M_{n_{min}}^2 \sim 0$ . Focusing on the turning points for large  $z$  (higher radial excitations), we obtain the following integral to the turning points:

$$z(V^*) = 2 \int_0^{V^*} \frac{dM^2}{\frac{dM^2}{dn} \sqrt{V^* - M^2}}. \quad (\text{B6})$$

Thus, we can infer the large  $z$  behavior of the potential near the turning points using just one RKR equation and then extract a dilaton.

- 
- [1] J. M. Maldacena, The Large N limit of superconformal field theories and supergravity, *Adv. Theor. Math. Phys.* **2**, 231 (1998), arXiv:hep-th/9711200.
- [2] J. Erdmenger, N. Evans, I. Kirsch, and E. Threlfall, Mesons in Gauge/Gravity Duals - A Review, *Eur. Phys. J. A* **35**, 81 (2008), arXiv:0711.4467 [hep-th].
- [3] J. Polchinski and M. J. Strassler, Deep inelastic scattering and gauge / string duality, *JHEP* **05**, 012, arXiv:hep-th/0209211.
- [4] H. Boschi-Filho and N. R. F. Braga, Wilson loops for a quark anti-quark pair in D3-brane space, *JHEP* **03**, 051, arXiv:hep-th/0411135.
- [5] J. Erlich, E. Katz, D. T. Son, and M. A. Stephanov, QCD and a holographic model of hadrons, *Phys. Rev. Lett.* **95**, 261602 (2005), arXiv:hep-ph/0501128.
- [6] H. Forkel, M. Beyer, and T. Frederico, Linear square-mass trajectories of radially and orbitally excited hadrons in holographic QCD, *JHEP* **07**, 077, arXiv:0705.1857 [hep-ph].
- [7] A. Karch, E. Katz, D. T. Son, and M. A. Stephanov, Linear confinement and AdS/QCD, *Phys. Rev. D* **74**, 015005 (2006), arXiv:hep-ph/0602229.
- [8] R. Rydberg, , *Z. Phys* **73**, 376 (1931).
- [9] R. Rydberg, , *Z. Phys* **80**, 514 (1933).
- [10] O. Klein, , *Z. Phys* **76**, 226 (1932).
- [11] A. L. G. Rees, , *Proc. Phys. Soc (London)* **59**, 998 (1947).
- [12] C. P. Herzog, A Holographic Prediction of the Deconfinement Temperature, *Phys. Rev. Lett.* **98**, 091601 (2007), arXiv:hep-th/0608151.
- [13] M. Kruczenski, D. Mateos, R. C. Myers, and D. J. Winters, Meson spectroscopy in AdS / CFT with flavor, *JHEP* **07**, 049, arXiv:hep-th/0304032.
- [14] J.-K. Chen, Regge trajectories for the mesons consisting of different quarks, *Eur. Phys. J. C* **78**, 648 (2018).
- [15] N. R. F. Braga, L. F. Ferreira, and A. Vega, Holographic model for charmonium dissociation, *Phys. Lett. B* **774**, 476 (2017), arXiv:1709.05326 [hep-ph].
- [16] M. A. Martin Contreras and A. Vega, Different approach to decay constants in AdS/QCD models, *Phys. Rev. D* **101**, 046009 (2020), arXiv:1910.10922 [hep-th].
- [17] A. Karch and E. Katz, Adding flavor to AdS / CFT, *JHEP* **06**, 043, arXiv:hep-th/0205236.
- [18] M. Ammon and J. Erdmenger, *Gauge/gravity duality: Foundations and applications* (Cambridge University Press, Cambridge, 2015).
- [19] H. Boschi-Filho and N. R. F. Braga, QCD / string holographic mapping and glueball mass spectrum, *Eur. Phys. J. C* **32**, 529 (2004), arXiv:hep-th/0209080.
- [20] R. L. Workman *et al.* (Particle Data Group), Review of Particle Physics, *PTEP* **2022**, 083C01 (2022).
- [21] R.-G. Cai and J. P. Shock, Holographic confinement/deconfinement phase transitions of AdS/QCD in curved spaces, *JHEP* **08**, 095, arXiv:0705.3388 [hep-th].
- [22] N. R. F. Braga, L. F. Faulhaber, and O. C. Junqueira, Confinement-deconfinement temperature for a rotating quark-gluon plasma, *Phys. Rev. D* **105**, 106003 (2022), arXiv:2201.05581 [hep-th].
- [23] C. A. Ballon Bayona, H. Boschi-Filho, N. R. F. Braga, and L. A. Pando Zayas, On a Holographic Model for Confinement/Deconfinement, *Phys. Rev. D* **77**, 046002 (2008), arXiv:0705.1529 [hep-th].
- [24] A. E. Bernardini and R. da Rocha, Entropic information of dynamical AdS/QCD holographic models, *Phys. Lett. B* **762**, 107 (2016), arXiv:1605.00294 [hep-th].
- [25] A. E. Bernardini, N. R. F. Braga, and R. da Rocha, Configurational entropy of glueball states, *Phys. Lett. B* **765**, 81 (2017), arXiv:1609.01258 [hep-th].
- [26] N. R. F. Braga and R. a. da Rocha, AdS/QCD duality and the quarkonia holographic information entropy, *Phys. Lett. B* **776**, 78 (2018), arXiv:1710.07383 [hep-th].
- [27] P. Colangelo and F. Loparco, Configurational Entropy can disentangle conventional hadrons from exotica, *Phys.*

- Lett. B **788**, 500 (2019), arXiv:1811.05272 [hep-ph].
- [28] L. F. Ferreira and R. da Rocha, Tensor mesons, AdS/QCD and information, *Eur. Phys. J. C* **80**, 375 (2020), arXiv:1907.11809 [hep-th].
- [29] L. F. Ferreira and R. da Rocha, Nucleons and higher spin baryon resonances: An AdS/QCD configurational entropic incursion, *Phys. Rev. D* **101**, 106002 (2020), arXiv:2004.04551 [hep-th].
- [30] R. da Rocha, Information entropy in AdS/QCD: Mass spectroscopy of isovector mesons, *Phys. Rev. D* **103**, 106027 (2021), arXiv:2103.03924 [hep-ph].
- [31] N. R. F. Braga, L. F. Ferreira, and R. a. Da Rocha, Thermal dissociation of heavy mesons and configurational entropy, *Phys. Lett. B* **787**, 16 (2018), arXiv:1808.10499 [hep-ph].
- [32] N. R. F. Braga and R. da Mata, Configuration entropy description of charmonium dissociation under the influence of magnetic fields, *Phys. Lett. B* **811**, 135918 (2020), arXiv:2008.10457 [hep-th].
- [33] N. R. F. Braga and R. da Mata, Configuration entropy for quarkonium in a finite density plasma, *Phys. Rev. D* **101**, 105016 (2020), arXiv:2002.09413 [hep-th].
- [34] N. R. F. Braga and O. C. Junqueira, Configuration entropy and confinement/deconfinement transition in holographic QCD, *Phys. Lett. B* **814**, 136082 (2021), arXiv:2010.00714 [hep-th].
- [35] M. A. Martin Contreras, A. Vega, and S. Diles, A holographic bottom-up description of light nuclide spectroscopy and stability, *Phys. Lett. B* **835**, 137551 (2022), arXiv:2206.01834 [hep-ph].
- [36] M. A. Martin Contreras and A. Vega, Holographic stability for non- $qq\bar{q}$  candidates, *Phys. Rev. D* **108**, 126024 (2023), arXiv:2309.02905 [hep-ph].
- [37] M. A. Martin Contreras, A. Vega, and S. Diles, Isospin and configurational entropy as testing tools for bottom-up AdS/QCD, *Phys. Lett. B* **854**, 138723 (2024), arXiv:2308.16007 [hep-ph].
- [38] X. Guo, M. A. Martin Contreras, X. Chen, and D. Xiang, A holographic bottom-up approach to  $\Sigma$  baryons, *Chin. Phys. C* **48**, 0462 (2024), arXiv:2404.16608 [hep-ph].
- [39] R. J. Le Roy, , *Journal of Quantitative Spectroscopy & Radiative Transfer* **186**, 158 (2017).